Minimum Shear Reinforcement for Columns with High-Strength Reinforcement and Concrete

Yu-Chen Ou, Aff.M.ASCE[1]; Harun Alrasyid[2]; and Nguyen Van Bao Nguyen[3]

Abstract: Large-scale reinforced concrete columns with high-strength reinforcement and concrete were tested. The nominal compressive strength of concrete was 70 MPa. The nominal yield strengths of longitudinal and shear reinforcement were 690 and 790 MPa, respectively. The columns were subjected to double-curvature lateral cyclic loading under constant axial compression. Test variables included the amount of shear reinforcement and level of axial compression. Test results showed that all the nine columns tested failed in shear and showed a successful redistribution of internal forces at diagonal cracking. The stress of shear reinforcement at the peak load increased with an increasing amount of shear reinforcement. Three of four columns with the highest amount of shear reinforcement (0.56%) showed yielding of shear reinforcement at the peak load. By comparing with the test results of 86 high-strength columns from this research and the literature, the minimum shear reinforcement equation of the ACI 318 code was found not able to prevent failure at diagonal cracking and failed to provide a clear trend between the reserve shear strength and the amount of shear reinforcement. A minimum shear reinforcement equation is thus proposed. The equation is based on the V_c equation of the ACI 318 code and can consider the effect of axial compression. Comparing 86 columns shows that the columns that failed at diagonal cracking do not satisfy the proposed equation. Moreover, the proposed equation can provide a clear trend between the reserve shear strength and the amount of shear reinforcement. **DOI: 10.1061/(ASCE)ST.1943-541X.0002854.**

Author keywords: Seismic; Columns; High-strength concrete; High-strength reinforcement; Shear; Diagonal cracking; Axial compression; Minimum shear reinforcement.

Introduction

As the population of urban areas increases, the need for high-rise buildings increases. High-rise buildings accommodate more residents per land area, allowing for an urban area to be planned with more green lands. Residents can thus enjoy a better living environment with better ventilation, sun lighting, and views than if the area is crowded with low-rise buildings. However, as the number of stories increases, the size of the columns and congestion of reinforcement increase due to increased gravity and seismic loads. To reduce the impact of large column dimensions on the available floor area and reinforcement congestion on construction, the use of high-strength concrete and reinforcement becomes necessary. To investigate the behavior of reinforced concrete (RC) with high-strength concrete and reinforcement, the Taiwan New RC project was initiated. This research is part of the project and is aimed at examining the minimum amount of shear reinforcement for columns with high-strength concrete and reinforcement.

Much research has been carried out in recent years to study the shear behavior of beams and columns using high-strength shear reinforcement. Six shear-critical beams with $f_{yt} = 690$ and 550 MPa were tested by Munikrishna et al. (2011). Test results showed that shear reinforcement yielded at the ultimate condition. The f_c' of the beams ranged from 32.5 to 40.3 MPa. Tests of 25 shear-critical beams with high-strength shear reinforcement having $f_{yt} = 555.3$–750.1 MPa (Lee et al. 2011, 2015) showed that shear reinforcement of most of the beams yielded at the ultimate condition. Some beams with a low f_c' did not show yielding of shear reinforcement. They were designed with $f_{yt} = 750.1$ MPa with $f_c' = 25$ MPa or $f_{yt} = 667$ MPa with $f_c' = 33.6$ MPa. These studies showed that high-strength shear reinforcement may not yield at the ultimate when f_c' is low. Two shear-critical columns with $f_{yt} =$ 735 MPa and $f_c' = 113.8$ MPa were tested by Kuramoto and Minami (1992). Two shear-critical columns with $f_{yt} = 875$ MPa and $f_c' = 72.1$ MPa were tested by Kuwada et al. (1993). In each of the two tests, one column was subjected to an axial compressive load of $0.17A_gf_c'$, and the other one was $0.33A_gf_c'$. The shear reinforcement ratio of all the four columns was 0.53%. The shear reinforcement of these four columns yielded at the peak applied shear. In contrast, ten shear-critical columns with $f_{yt} = 846$ MPa and $f_c' = 57.1$ MPa were tested by Seo and Noguch (1992). Seven columns were subjected to an axial compressive load of $0.3A_gf_c'$, while the other three were 0, 0.15, and $0.6A_gf_c'$. Shear reinforcement ratios ranged from 0.3% to 1.8%. No yielding of shear reinforcement was observed at the peak load. Since the columns tested in these studies were rather small with a dimension 200×200 mm or 300×300 mm. Column specimens with a dimension of 600×600 mm were recently studied by Ou and Kurniawan (2015a, b). A total of 16 columns with $f_{yt} = 862$ MPa and

[1]Distinguished Professor, Dept. of Civil Engineering, National Taiwan Univ., No. 1, Section 4, Roosevelt Rd., Taipei 106, Taiwan (corresponding author). ORCID: https://orcid.org/0000-0001-5779-3943. Email: yuchenou@ntu.edu.tw

[2]Assistant Professor, Dept. of Civil Engineering, Sepuluh Nopember Institute of Technology, ITS Campus, Keputih, Sukolilo Surabaya 60111, Indonesia. Email: harun@ce.its.ac.id

[3]Lecturer, Dept. of Civil Engineering, Univ. of Danang—Univ. of Technology and Education, 48 Cao Thang St., Danang 550000, Vietnam; Ph.D. Candidate, Dept. of Civil Engineering, National Taiwan Univ., No. 1, Section 4, Roosevelt Rd., Taipei 106, Taiwan. Email: nvbnguyen@ute.udn.vn

Note. This manuscript was submitted on January 22, 2020; approved on July 17, 2020; published online on November 18, 2020. Discussion period open until April 18, 2021; separate discussions must be submitted for individual papers. This paper is part of the ***Journal of Structural Engineering***, © ASCE, ISSN 0733-9445.

$f_c' = 92.5$–130 MPa were tested. Shear reinforcement ratio ranged from 0.14% to 0.24%. Test results showed that the shear reinforcement of all the columns did not yield at the peak load. However, it was also observed that the stress of shear reinforcement increased with an increasing amount of shear reinforcement. The studies on columns mentioned showed that high-strength shear reinforcement when used in columns may not yield even with the use of high-strength concrete. The results of the tests by Ou and Kurniawan (2015a, b) also showed that columns with high axial compression failed right at diagonal cracking even though the amount of shear reinforcement satisfied the minimum shear reinforcement requirement of the ACI 318 code. It was shown with increasing axial compression, the diagonal cracking strength tended to increase, likely increasing the internal forces that needed to be redistributed at the diagonal cracking. More shear reinforcement was likely needed for a successful redistribution of internal forces to avoid failure right at diagonal cracking. However, the current minimum shear reinforcement equations of the ACI 318-19 code does not consider the effect of axial compression.

In this research, large-scale shear-critical column specimens were tested. Longitudinal and shear reinforcement had a specified yield strength of 690 and 790 MPa, respectively. The specified concrete compressive strength was 70 MPa. This research is a continuation of previous studies conducted by Ou and Kurniawan (2015a, b). Columns with more shear reinforcement were tested in this research. The main objective of this research is to investigate the effect of axial compression and the amount of shear reinforcement on the shear behavior of high-strength columns, particularly on the stress of shear reinforcement at the peak load and failure modes of columns. Moreover, a new minimum shear reinforcement equation that can consider the effect of axial compression to ensure a successful redistribution of internal forces at diagonal cracking is proposed.

Experimental Program

Specimen Design and Test Set Up

A total of 10 columns were tested. The dimension and reinforcement design of the specimens are shown in Fig. 1, and the important values of design parameters are listed in Table 1. All the columns had a cross section of 600 × 600 mm and a clear height of 1,800 mm. The actual yield strength of longitudinal reinforcement (f_{yl}) and shear reinforcement (f_{yt}) were 735 and 862 MPa, respectively. The actual compressive strength of concrete (f_c')

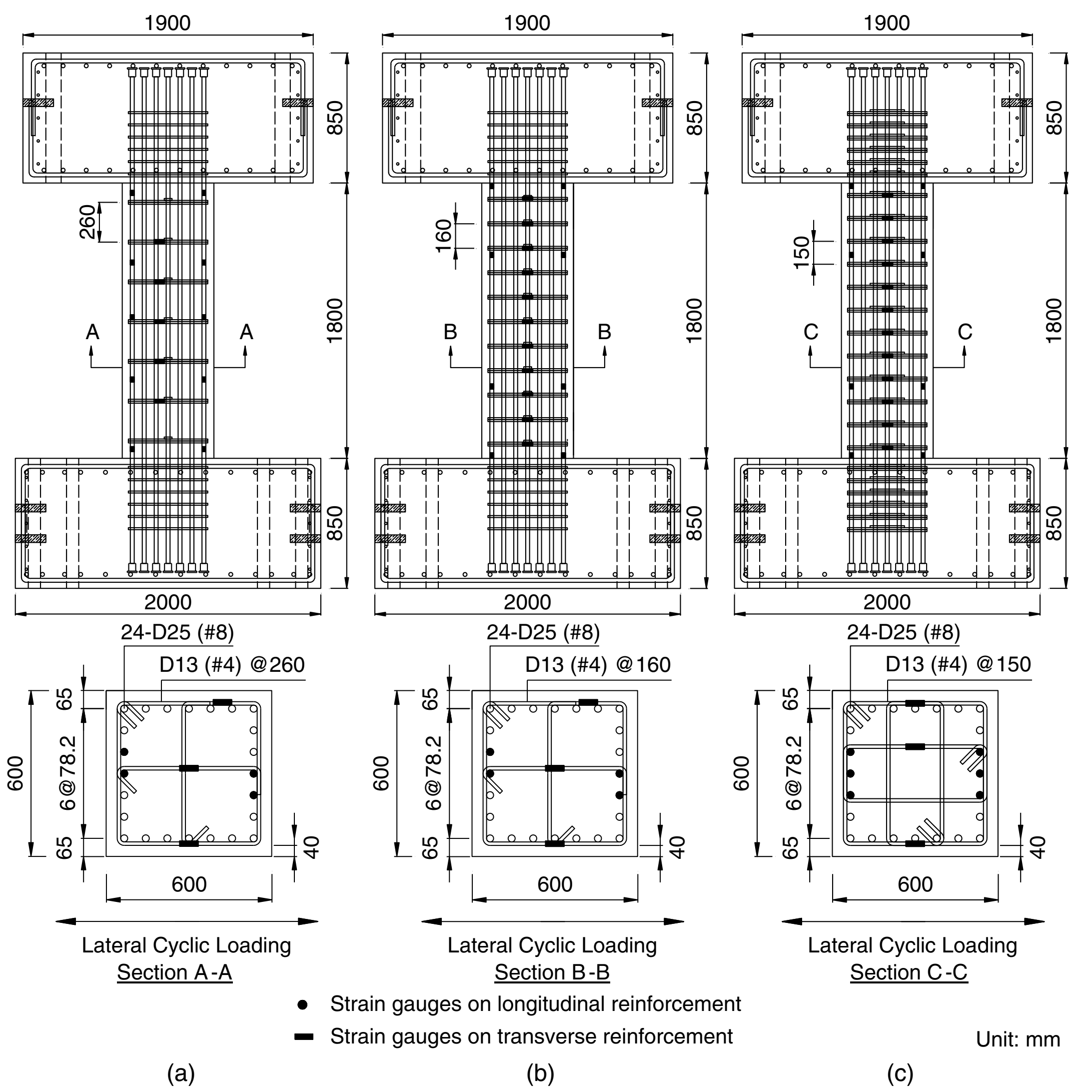

Fig. 1. Column design: (a) A-3.1, B-3.1; (b) A-5, B-5, C-5, D-5; and (c) A-6, B-6, C-6 D-6.

J. Struct. Eng., 2021, 147(2): 04020313

Table 1. Column design parameters

Column	Axial compression ratio, $N_u/A_g f'_c$ (%)	Axial compression load (kN)	Concrete compressive strength, f'_c (MPa)	Longitudinal reinforcement, D25(#8)		Shear reinforcement, D13(#4)		
				f_{yl} (MPa)	ρ_l (%)	f_{yt} (MPa)	s (mm)	ρ_t (%)
A-3.1		3,319	92.2				260	0.24
A-5	10	2,531	70.3				160	0.40
A-6		3,268	90.8				150	0.56
B-3.1		5,616	78.0				260	0.24
B-5	20	5,616	78.0	735	3.38	862	160	0.40
B-6		7,279	101.1				150	0.56
C-5	30	8,597	79.6				160	0.40
C-6		8,672	80.3				150	0.56
D-5	40	11,923	82.8				160	0.40
D-6		12,226	84.9				150	0.56

ranged from 78.0 to 101.1 (Table 1). The design variables of the columns were the axial compression and amount of shear reinforcement. Four levels of axial compression were studied, i.e., 10%, 20%, 30%, and 40%$A_g f'_c$. This is the same as in the previous research by Ou and Kurniawan (2015a, b). Based on the level of axial compression, the columns are referred to as series A, B, C, and D columns, respectively. The amounts of shear reinforcement (ρ_t) examined in the previous research were 0.14% and 0.24%. In this research, the amounts were increased to investigate the minimum amount of shear reinforcement to ensure the successful redistribution of internal forces at diagonal cracking. In this research, the amounts of shear reinforcement in series A and B columns were 0.24%, 0.40%, and 0.56%; while those of series C and D were 0.40% and 0.56%. In the previous research, D32 (No. 10) bars were used for longitudinal reinforcement. In this research, they were replaced with D25 (No. 8) bars because D32 was not available. However, the amount of longitudinal reinforcement remained similar. It was 3.52% and 3.38% in the previous and this research. The columns were tested using the multiaxial testing system (MATS) (Fig. 2) at the National Center for Research on Earthquake Engineering (NCREE), Taiwan. The columns were tested by lateral double-curvature loading under a constant axial compression to simulate the loading condition of a column in a moment-resisting frame under gravity and seismic loads. During testing, an axial compression according to the value in Table 1 was applied first through hydraulic jacks beneath the steel floor supporting the column. The axial compression remained constant throughout the testing. Lateral cyclic loading was later applied using displacement control to drift levels of 0.25%, 0.375%, 0.5%, 0.75%, 1.0%, 1.5%, 2.0%, 3.0%, 4.0%, and 5.0%. Each drift level was repeated three times. Note that the peak drift that was actually achieved was less because of the gaps between the actuator and the column. Actual drifts are used in the following sections.

Test Results and Discussion

Damage Progress and Failure Modes

For series A columns, only columns A-3.1 and A-6 are presented herein because testing of A-5 was not successful due to the inappropriate installation of the column in the testing machine. For columns A-3.1 and A-6, as the lateral load increased, flexural cracks near two ends appeared first, followed by flexural-shear cracks extended from the flexural cracks and then by web-shear cracks distributed over almost the entire height of the column. Column A-6 with 0.56% shear reinforcement showed a denser distribution of cracks at the peak load than A-3.1 [Figs. 3(a and b)]. After the peak load, diagonal cracks started to widen, eventually leading to the crushing of concrete along diagonal cracks [Figs. 4(a and b)].

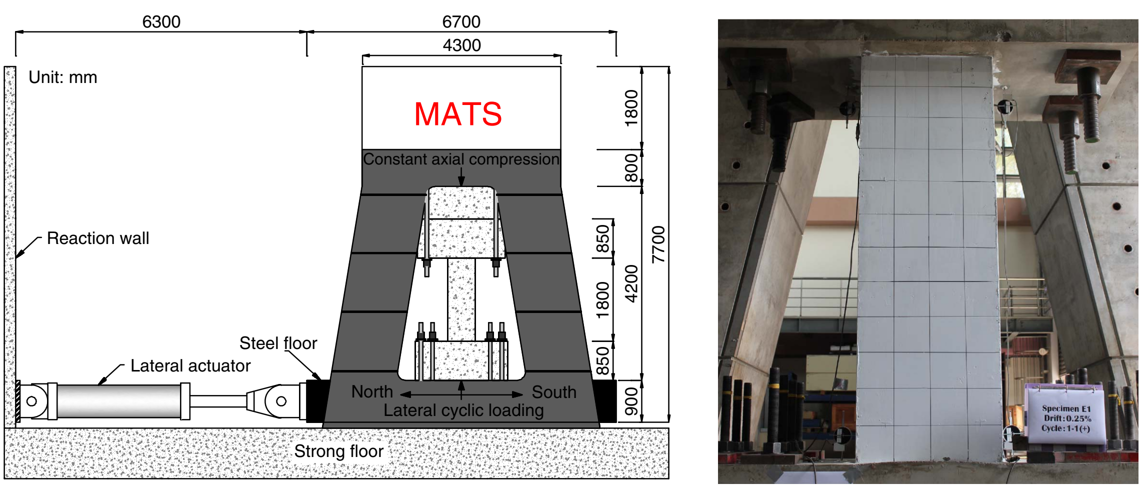

(a) (b)

Fig. 2. (a) Multiaxial testing system (MATS); and (b) photograph of the test setup.

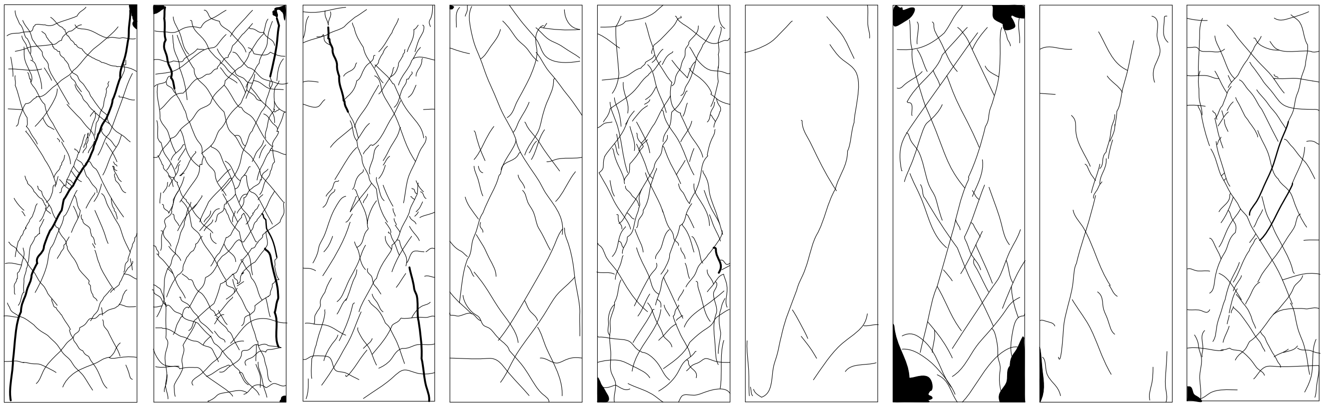

(a) (b) (c) (d) (e) (f) (g) (h) (i)

Fig. 3. Crack pattern at the ultimate condition (peak load) for columns: (a) A-3.1; (b) A-6; (c) B-3.1; (d) B-5; (e) B-6; (f) C-5; (g) C-6; (h) D-5; and (i) D-6.

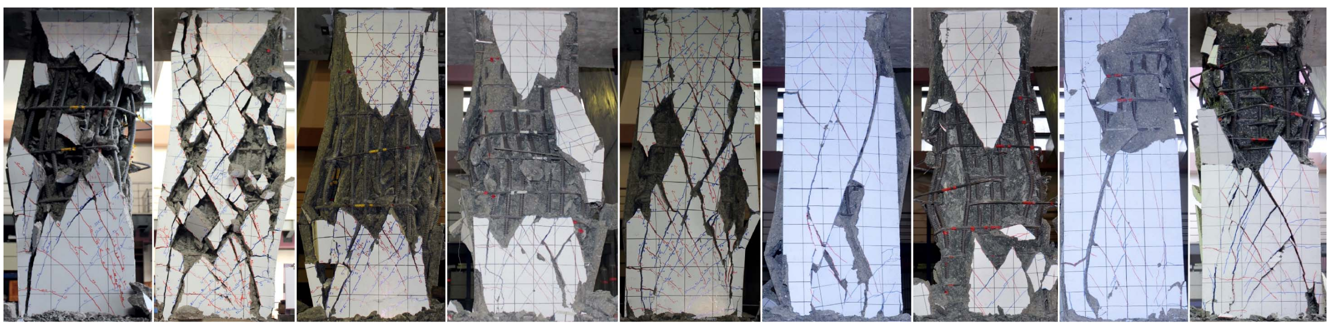

(a) (b) (c) (d) (e) (f) (g) (h) (i)

Fig. 4. Damage columns at the end of test: (a) A-3.1; (b) A-6; (c) B-3.1; (d) B-5; (e) B-6; (f) C-5; (g) C-6; (h) D-5; and (i) D-6.

The failure mode of both columns is shear failure. The lateral loads of both columns continued increasing after diagonal cracking, indicating a successful redistribution of internal forces at diagonal cracking. The reserve shear strength ratios (α), defined as the ratio of the ultimate shear strength (peak load) to the diagonal cracking strength, of columns A-3.1 and A-6 are 1.31 and 1.85, respectively (Table 2). The ratio increased with an increasing amount of shear reinforcement because the diagonal cracking strength remained similar, but the ultimate shear strength increased due to increasing contribution from shear reinforcement. The ratios for both columns are larger than one. This type of shear failure is referred to as type A as illustrated in Fig. 5(a).

For series B columns, as the load increased, flexural cracks occurred generally later than series A columns due to higher axial compression. Flexural-shear and web-shear cracks appeared almost simultaneously. Series B columns showed a higher diagonal cracking strength than corresponding series A columns (B-3.1 versus A-3.1 and B-6 versus A-6) (Table 2) and exhibited a less number of cracks at peak load [Figs. 3(c–e)]. Failure of series B columns was shear failure due to the widening of diagonal cracks, leading to crushing of concrete along the cracks [Figs. 4(c–e)] and buckling of longitudinal reinforcement. Column B-3.1 showed diagonal cracking during the drift cycles with a peak drift of 0.52%. The peak load of B-3.1 also occurred during the same drift

Table 2. Shear strengths at the diagonal cracking and ultimate condition (peak load)

Column	Diagonal cracking				Ultimate condition (peak load)						
	Drift ratio (%)	σ_{yt} (MPa)	V_{test_d} (kN)	σ_{yl} (MPa)	Drift ratio (%)	σ_{yt} (MPa)	V_{test_u} (kN)	σ_{yl} (MPa)	α	Type of failure	V_{Mn} (kN)
A-3.1	0.37	50	1,382	347	0.84	329	1,817	496	1.31	A	2,573
A-6	0.37	17	1,339	258	1.82	862	2,480	690	1.85	A	2,558
B-3.1	0.28	37	1,999	198	0.52	506	1,999	451	1.00	B	2,678
B-5	0.48	52	2,010	341	0.68	642	2,195	380	1.09	A	2,678
B-6	0.50	64	2,197	293	1.19	592	2,856	494	1.30	A	3,079
C-5	0.55	42	2,400	311	0.55	394[a]	2,400	311	1.00	B	2,636
C-6	0.72	26	2,689	445	1.19	862	3,039	735	1.13	A	2,633
D-5	0.49	25	2,560	218	0.49	569[a]	2,560	218	1.00	B	2,618
D-6	0.52	173	2,341	335	0.75	862	2,535	473	1.08	A	2,647

[a]Stress of shear reinforcement measured at a drift next to the ultimate drift (peak load).

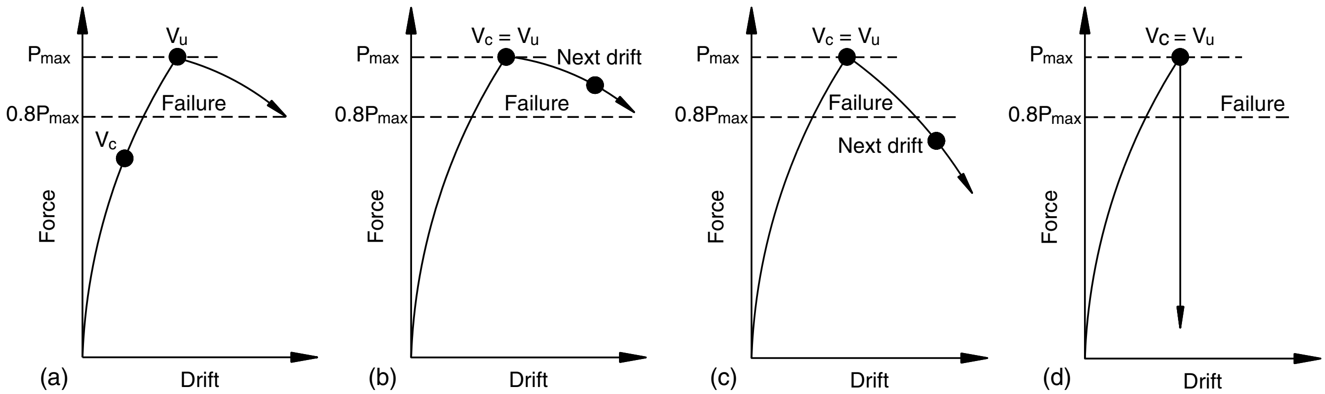

Fig. 5. Types of shear failure: (a) Type A; (b) Type B; (c) Type C; and (d) Type D.

cycles (0.52%). Therefore, the reserve shear strength ratio of B-3.1 is 1.00. However, the column did not fail during this drift of loading. The internal forces of the column were successfully redistributed at the diagonal cracking. The column continued sustaining a lateral load more than 80% of the peak load in the next drift of loading (0.77%). This type of shear failure is referred to as type B, as illustrated in Fig. 5(b). For columns B-5 and B-6, the lateral load continued increasing after the drift level in which diagonal cracking occurred. The reserve shear strength ratios of B-5 and B-6 are 1.09 and 1.30, respectively. The failure of B-5 and B-6 is classified as type A shear failure. The reserve shear strength ratios of series B columns are less than the corresponding series A columns (e.g., B-3.1 versus A-3.1 and B-6 versus A-6) (Table 2). The ratios reduced because the diagonal cracking strength increased due to increased axial compression, while the shear strength contribution from shear reinforcement to the ultimate shear strength appeared to decrease (Table 2).

Due to the increase of the axial compression, series C columns showed fewer cracks than corresponding series B columns [Figs. 3(f and g)]. For column C-5, no flexural cracks were observed before diagonal cracking. Flexure, flexural-shear, and web-shear cracks appeared simultaneously during the same drift loading (0.55%), and the column reached the peak load at the same drift. However, the column did not fail and was able to take a lateral load more than 80% of the peak load in the next drift level of loading (0.82%). The failure mode is type B shear failure. Column C-5 eventually failed at a drift of 1.1% due to the widening of diagonal cracks, leading to the crushing of concrete and buckling of longitudinal reinforcement [Fig. 4(f)]. For column C-6, flexure, flexural-shear, and web-shear cracks occurred consecutively. More cracks appeared at the peak load than C-5. Column C-6 failed in a way [Fig. 4(g)] similar to C-5 except that the toes at the two ends of column C-6 showed more spalling due to a higher moment developed by a higher amount of shear reinforcement, delaying shear failure. The lateral load of column C-6 continued increasing after diagonal cracking. The reserve shear strength ratio is 1.13, and the failure mode is classified as type A shear failure.

For column D-5, due to a further increased axial compression, flexural-shear cracks did not appear. Flexural and web-shear cracks occurred simultaneously during the drift loading of 0.49%. The column reached the peak load during the same drift loading. However, the column was able to take a lateral load larger than 80% of the peak load in the next drift level of loading (0.77%). The column eventually failed due to the widening of shear cracks, leading to crushing and spalling of concrete along the cracks and buckling of longitudinal reinforcement [Fig. 4(h)]. The failure mode is classified as type B shear failure. Column D-6 with more shear reinforcement than D-5 showed more cracks [Fig. 3(i)]. For this column, flexure, flexural-shear, and web-shear cracks appeared consecutively. The lateral load continued increasing in the drift level (0.75%) next to the drift with diagonal cracking (0.52%). The failure mode is type A shear failure. The column eventually failed due to the widening of shear cracks and the crushing of concrete [Fig. 4(i)] similar to D-5.

Lateral Force and Displacement Relationships

Figs. 6(a and b) show the lateral force and displacement relationships of the columns. Note that the $P-\Delta$ effect due to the lateral movement of the applied axial load has been removed from the plots. Important events including flexural cracking, shear cracking, and peak load are indicated in the plots. The strengths of all the columns generally dropped rapidly after the peak load. This is typical of shear failure. Increasing the amount of shear reinforcement slowed down the degradation of the strength after the peak (from A-3.1 to A-6, B-3.1 to B-5, C-5 to C-6, and D-5 to D-6). The column became more ductile. In contrast, increasing axial compression tended to increase the degradation of the strength after the peak load and the column tended to fail more suddenly at a higher load (from A-6 to D-6, and from B-5 to D-5). The behavior became more brittle and failed more abruptly.

Diagonal Cracking Strength and Ultimate Shear Strength

The diagonal cracking strength V_{test_d} and ultimate shear strength V_{test_u} for each column are listed in Table 2. Note that V_{test_d} includes a small contribution from shear reinforcement. The contribution is small because the maximum stress of shear reinforcement at diagonal cracking is small, as listed in the third column of Table 2. Table 2 shows that V_{test_d} increases with increasing axial compression for series A, B, and C columns. However, the increase in percentage decreases with increasing axial compression. From series A to B columns, the average increase percentage is 52%, while from series B to C columns, the average increase percentage is 23%. When the axial compression is increased to the level of series D columns, the V_{test_d} increases only slightly (C-5 to D-5) or even decreases (C-6 to D-6). The average increase rate is −4%, meaning there is a decrease. This phenomenon confirms again axial compression is beneficial to diagonal cracking strength when it is low. Axial compression turns detrimental to diagonal cracking strength when it is high. This is because at high axial compression the weakening effect of axial compression on diagonal tensile

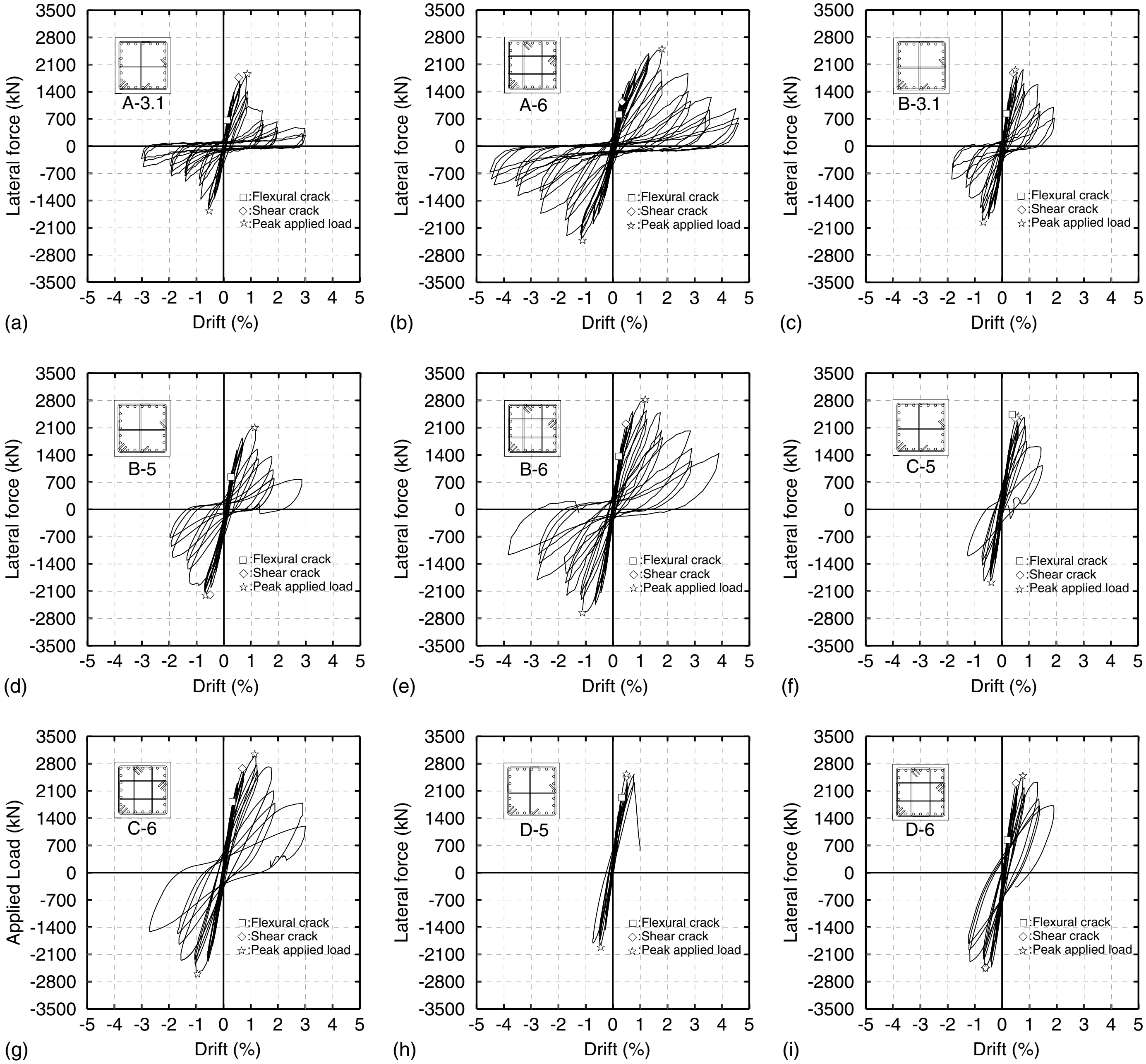

Fig. 6. Lateral force and displacement relationships: (a) A-3.1; (b) A-6; (c) B-3.1; (d) B-5; (e) B-6; (f) C-5; (g) C-6; (h) D-5; and (i) D-6.

strength is more than the decreasing effect of axial compression on diagonal tension demand (Ou and Kurniawan 2015a). The decrease of diagonal tensile strength is more than the decrease of diagonal tensile demand. Table 2 also shows that the diagonal cracking strength is not significantly affected by the amount of shear reinforcement.

A similar trend can be seen for the ultimate shear strength (Table 2). With increasing axial compression, the ultimate shear strength first increases and then decreases. For example, from A-6 to B-6, from B-6 to C-6, and from C-6 to D-6, the percentage increase of the ultimate shear strength is 15%, 6%, and −17%. It appears that the beneficial effect of axial compression on the ultimate shear strength is only for axial compression up to $30\%A_g f'_c$. The positive effect disappears and turns negative when axial compression increases to $40\%A_g f'_c$. This observation is consistent with Ou and Kurniawan (2015a).

Stress of Longitudinal and Shear Reinforcement

The maximum stresses of longitudinal and shear reinforcement at the diagonal cracking condition and at the ultimate condition (peak load) are listed in Table 2. The table shows that longitudinal reinforcement did not yield at the diagonal cracking for all the columns. At the peak load condition, only the longitudinal reinforcement of column C-6 yielded. For this column, the peak load is larger than the shear corresponding to the nominal moment strength of the column calculated based on actual material strengths (The last column of Table 2). Therefore, the failure mode of column C-6 is a shear failure after reaching the nominal moment strength. The maximum stresses of shear reinforcement of all the columns were small right before diagonal cracking as listed in the third column of Table 2. The stresses increased rapidly after diagonal cracking. At the ultimate condition (peak load), many of the columns did not show yielding of shear reinforcement. However, the

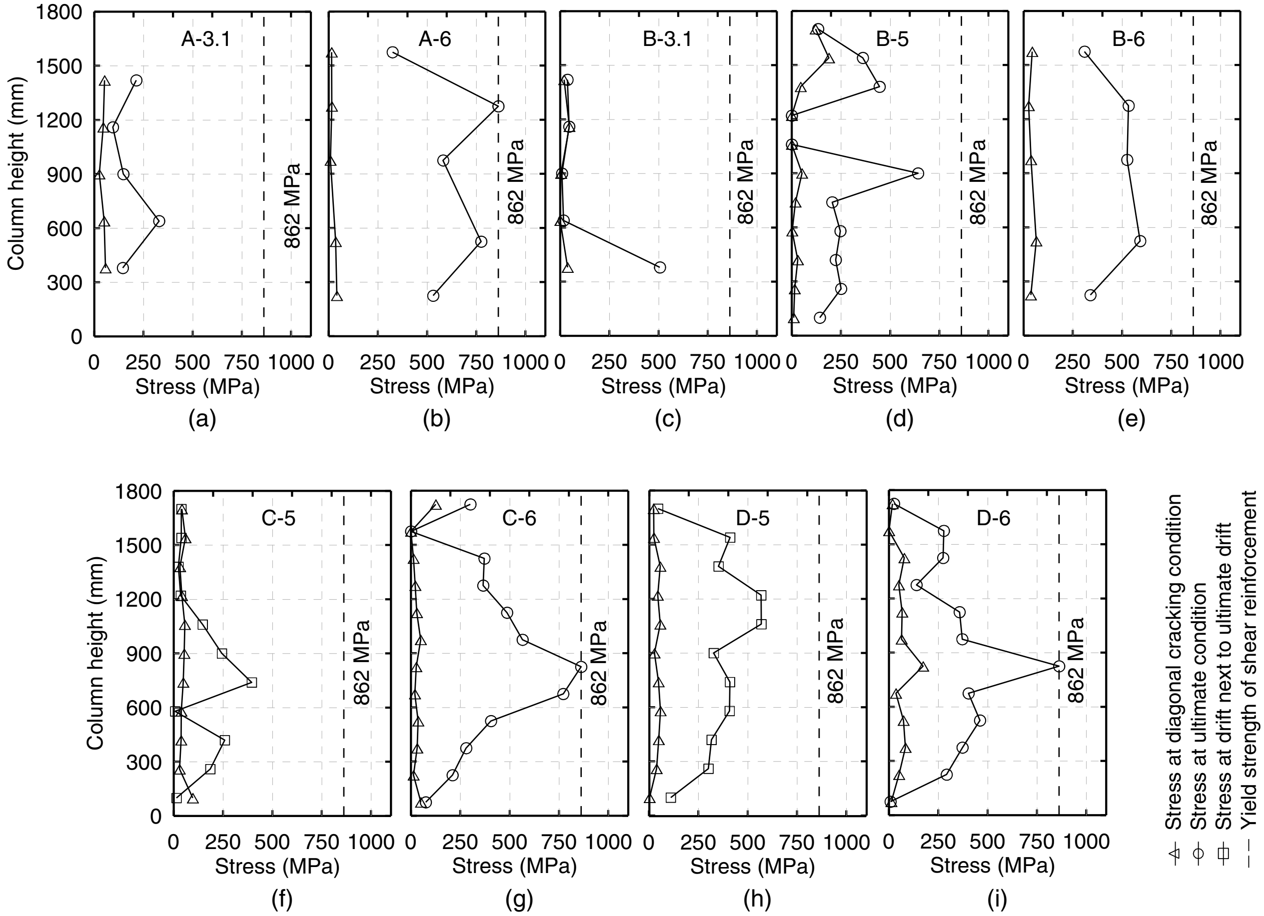

Fig. 7. Stress distribution of shear reinforcement: (a) A-3.1; (b) A-6; (c) B-3.1; (d) B-5; (e) B-6; (f) C-5; (g) C-6; (h) D-5; and (i) D-6.

results show that the maximum stress of shear reinforcement tended to increase with increasing shear reinforcement. Columns with the highest amount of shear reinforcement, 0.56%, showed yielding of shear reinforcement at the ultimate condition except for column B-6. Fig. 7 shows the distribution of the stress of shear reinforcement along the height of the column at the diagonal cracking and ultimate conditions. The yield stress, 862 MPa, is also shown in the plots. Note that more strain gauges were applied in series C and D columns than series A and B columns. Denser strain data are shown in Fig. 7 for series C and D columns. Moreover, the strain gauges were applied on the legs of shear reinforcement at or nearby the centroidal axis of the column section (Fig. 1). Strain gauges may not capture the maximum stress of shear reinforcement particularly when shear cracks are far away from the gauges.

Examination of Minimum Shear Reinforcement Equations

Minimum Shear Reinforcement Equation of ACI 318-19

The types of shear failure of the 9 columns tested in this research and 16 columns tested previously (Ou and Kurniawan 2015a, b) are listed in Table 3 according to the classification shown in Fig. 5. Columns of failure types of A and B do not fail right at the diagonal cracking and still can show a shear strength more than 80% of the peak strength at the next drift level. They are considered to have an acceptable behavior of shear failure. The amount of shear reinforcement is sufficient to allow successful redistribution of internal forces at diagonal cracking. All the columns tested in this research showed either type A or B behavior. Columns of failure type C do not fail right at the diagonal cracking but cannot sustain a lateral load more than 80% of the peak load at the next drift level. The columns are considered to fail at the same drift as diagonal cracking. Columns C-4 and D-1 to D-4 in the previous research (Ou and Kurniawan 2015a) showed this type of failure mode. Columns of failure type D fail right at the moment of diagonal cracking. Columns C-1 and C-2 in the previous research (Ou and Kurniawan 2015a) showed this type of failure mode. Failure types C and D lack warning at failure and hence are considered not acceptable. The amount of shear reinforcement should be increased for columns with failure types of C and D.

To ensure a warning of failure, a minimum amount of shear reinforcement as calculated by Eq. (1) or Eq. (2) is required by the ACI code [ACI 318 (ACI 2019)] for columns when the factored shear is more than half the design shear strength provided by concrete. The ratios of provided to required amounts of shear reinforcement ($\rho_t/\rho_{t,minACI}$) of all the 25 columns tested in this research and previous research (Ou and Kurniawan 2015a, b) are listed in Table 3. The ratios of all the columns are larger than one, meaning the amounts of shear reinforcement all satisfy the minimum requirement of the ACI 318 code. All series A and B columns showed acceptable failure types (A or B). However, many series C and D columns showed unacceptable failure types (C or D). For example, column C-1 with a provided amount 1.22 times the amount required by the ACI code showed a failure type of D,

J. Struct. Eng., 2021, 147(2): 04020313

Table 3. Examination of minimum shear reinforcement equations using 25 columns

Column	$\frac{\rho_t}{\rho_{t,minACI}}$	$\frac{\rho_t}{\rho_{t,min,p}}$	Type of failure	α	Column	$\frac{\rho_t}{\rho_{t,minACI}}$	$\frac{\rho_t}{\rho_{t,min,p}}$	Type of failure	α
A-1	1.30	0.67	A	1.25	C-1	1.22	0.31	D	1.00
A-2	1.23	0.62	A	1.27	C-2	1.06	0.24	D	1.00
A-3	2.20	1.12	A	1.39	C-3	2.11	0.53	A	1.03
A-4	2.09	1.04	A	1.37	C-4	1.90	0.44	C	1.00
A-3.1	2.25	1.16	A	1.31	C-5	3.94	1.09	B	1.00
A-6	5.24	2.71	A	1.85	C-6	5.58	1.53	A	1.13
B-1	1.20	0.48	A	1.12	D-1	1.24	0.25	C	1.00
B-2	1.12	0.37	A	1.14	D-2	1.11	0.21	C	1.00
B-3	2.03	0.66	A	1.15	D-3	2.09	0.42	C	1.00
B-4	1.96	0.62	A	1.20	D-4	1.91	0.35	C	1.00
B-3.1	2.45	0.90	B	1.00	D-5	3.86	0.85	B	1.00
B-5	3.98	1.46	A	1.09	D-6	5.42	1.18	A	1.08
B-6	4.97	1.67	A	1.30	—	—	—	—	—

meaning failure right at diagonal cracking. Column D-4 with a provided amount of 1.91 times the amount required by the code showed a failure type of C. As stated previously, the diagonal cracking strength increases with increasing axial compression. This increases the internal force that needs to be redistributed at diagonal cracking. However, the current equation of the minimum shear reinforcement in the ACI code [Eq. (1) or Eq. (2)] does not consider this effect of axial compression. The current equation only considers the effects of concrete compressive strength (f'_c) and yield strength of shear reinforcement (f_{yt})

$$A_{v,minACI} = 0.062\sqrt{f'_c}\frac{b_w s}{f_{yt}} \geq \frac{0.35 b_w s}{f_{yt}} \text{ (MPa)} \tag{1}$$

$$\rho_{t,minACI} = \frac{A_{v,minACI}}{b_w s} = 0.062\frac{\sqrt{f'_c}}{f_{yt}} \geq \frac{0.35}{f_{yt}} \text{ (MPa)} \tag{2}$$

Proposed Minimum Shear Reinforcement Equation

To ensure successful redistribution of internal forces at diagonal cracking, the minimum shear reinforcement should provide a shear strength that is proportional to the diagonal cracking strength. Since in the ACI 318 code the diagonal cracking strength is represented by V_c, the shear strength provided by the minimum shear reinforcement should be proportional to V_c. It is therefore proposed that the shear strength provided by the minimum shear reinforcement should be approximately equal to $0.365V_c$ as defined by Eq. (3). The V_c in Eq. (3) is from ACI 318-19 (ACI 2019) and includes the effect of axial compression as defined in Eq. (4). Combining Eqs. (3)–(5) and considering the current minimum shear reinforcement equation as the lower bound leads to the proposed minimum shear reinforcement equation as defined by Eq. (6) or Eq. (7). The coefficient in Eq. (3) is chosen so that when axial compression is zero ($N_u = 0$), the proposed equation [Eq. (6) or Eq. (7)] turns back to the current minimum shear reinforcement equation [Eq. (1) or Eq. (2)]. The maximum value of f_{yt} in Eqs. (6) and (7) is set as 550 MPa according to ACI 318-19 for seismic design

$$V_{s,min,p} = \frac{0.062}{0.17}V_c \approx 0.365V_c \tag{3}$$

$$V_c = \left(0.17\sqrt{f'_c} + \frac{N_u}{6A_g}\right) b_w d \text{ (MPa)} \tag{4}$$

$$V_{s,min,p} = \frac{A_{v,min,p} f_{yt} d}{s} \tag{5}$$

$$A_{v,min,p} = 0.062\left(\sqrt{f'_c} + \frac{N_u}{1.02A_g}\right)\frac{b_w s}{f_{yt}} \geq A_{v,minACI} \text{ (MPa)} \tag{6}$$

$$\rho_{t,min,p} = 0.062\left(\sqrt{f'_c} + \frac{N_u}{1.02A_g}\right)\frac{1}{f_{yt}} \geq \rho_{t,minACI} \text{ (MPa)} \tag{7}$$

d is taken as 80% of the full height of the cross section h.

The ratios of provided to required (by the proposed equation) amounts of shear reinforcement ($\rho_t/\rho_{t,min,p}$) of all the 25 columns are listed in Table 3. The results show that the ratios ($\rho_t/\rho_{t,min,p}$) of all the seven columns with unacceptable failure modes (C-1, C-2, C-4, D-1 to D-4) are much lower than one (≤0.5). In other words, these columns do not have a sufficient amount of shear reinforcement based on the proposed equation. This matches the failure modes of these columns. For those that showed acceptable failure modes, the proposed equation appears to be quite conservative for some columns subjected to low axial compression. For example, column B-1 and B-2 have the ratios ($\rho_t/\rho_{t,min,p}$) of 0.48 and 0.37, respectively, but still showed a failure mode of type A. Note again that the proposed equation becomes the current minimum shear reinforcement equation when the axial compression is zero.

A test database was established from the literature (Akihiko et al. 1990; Aoyama 2001; Kuramoto and Minami 1992; Maruta 2008; Ou and Kurniawan 2015a, b; Sakaguchi et al. 1990; Shinohara et al. 2008; Sibata et al. 1997; Takaine et al. 2010; Takami and Yoshioka 1997). The database contains 86 shear-critical high-strength columns. The major design parameters are listed in Appendix. The values of α (reserve shear strength ratio), $\rho_t/\rho_{t,minACI}$, and $\rho_t/\rho_{t,min,p}$ (proposed), of all the 86 columns were calculated and are listed in Appendix. Fig. 8(a) shows the relationship between α and $\rho_t/\rho_{t,minACI}$ of all the columns. The figure shows there is no clear trend between α and $\rho_t/\rho_{t,minACI}$, particularly for columns with high axial compression. The results also show that 12 columns with $\rho_t/\rho_{t,minACI} > 1.0$ have $\alpha = 1.0$. Many of which do not have successful redistribution of internal forces at diagonal cracking (e.g., C-1, C-2, C-4, D-1 to D-4). This means the minimum amount of shear reinforcement of the ACI code cannot prevent failure at diagonal cracking. Fig. 8(b) shows the relationship between α and $\rho_t/\rho_{t,min,p}$ of all the columns. A clear trend can be seen. The reserve shear strength ratio α increases with increasing value of $\rho_t/\rho_{t,min,p}$. Most of the columns with $\alpha = 1.0$ fall into the second quadrant, meaning they do not satisfy the proposed minimum shear reinforcement equation. There is only one column with

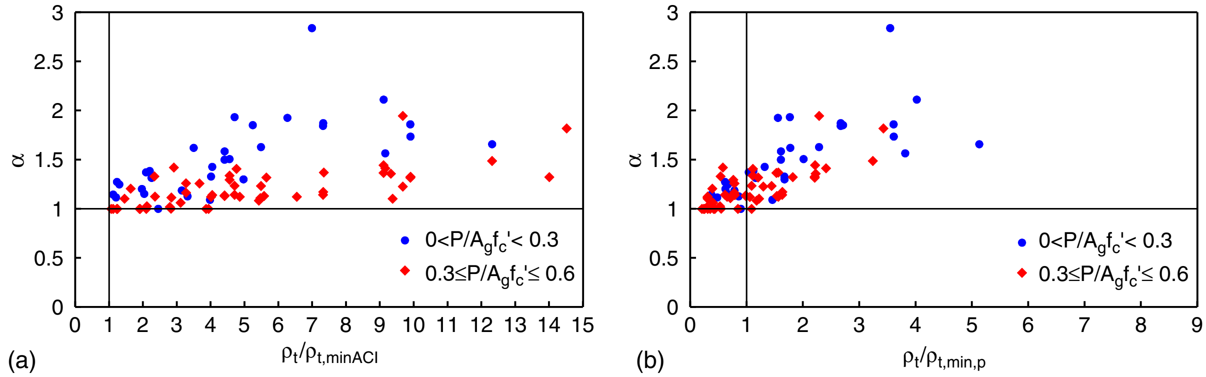

Fig. 8. Examination using 86 high-strength columns: (a) ACI 318-19 minimum shear reinforcement equation; and (b) proposed minimum shear reinforcement equation.

$\alpha = 1.0$ but still in the first quadrant. The column is C-5, which has $\rho_t/\rho_{t,min,p} = 1.09$. The failure mode of this columns is type B (Table 3), which is considered acceptable, as stated previously. Some columns with $\alpha > 1.0$ still fall into the second quadrant, meaning the proposed equation is conservative. Note that the proposed equation has been validated only by columns with high-strength reinforcement and concrete. Its applicability to normal-strength columns has yet to be investigated.

Summaries and Conclusions

Large-scale shear-critical columns with high-strength reinforcement and concrete were tested in this research. This research is a continuation of previous studies by Ou and Kurniawan (2015a, b). Test results of this research and those from previous studies were used to investigate the minimum shear reinforcement required for successful redistribution of internal forces at diagonal cracking. Important conclusions are summarized as follows.

1. All the nine columns tested in this research showed shear failure. The behavior of the columns turned more brittle with increasing axial compression and decreasing amount of shear reinforcement. All the nine columns showed acceptable shear failure modes, i.e., no columns failed at the same drift as the diagonal cracking. The shear reinforcement was sufficient to allow successful redistribution of internal forces at diagonal cracking.
2. All columns tested in this research reached the peak load without yielding of longitudinal reinforcement except for column C-6, which failed in shear after nominal moment strength was reached. Many of the columns reached the peak load without yielding of shear reinforcement. However, the stress of shear reinforcement tended to increase with an increasing amount of shear reinforcement. Three of the four columns with the highest amount of shear reinforcement (0.56%) reached the peak load with yielding of shear reinforcement.
3. From 25 columns tested in this research and previous research by Ou and Kurniawan (2015a, b), it was found that many of the columns with high axial compression ($30\% - 40\% A_g f'_c$) showed unacceptable failure modes, i.e., failure at the same drift as diagonal cracking, even though the provided amount of shear reinforcement satisfied the minimum shear reinforcement equation of the ACI 318 code. Moreover, from a database of 86 high-strength columns, by using the minimum shear reinforcement equation of the ACI 318 code, no clear trend was observed between the reserve shear strength and the ratio of provided to the required amount of shear reinforcement, particularly for columns with high axial compression ($\geq 30\% A_g f'_c$). To address this issue, a minimum shear reinforcement equation is proposed based on the V_c equation of the ACI 318-19 code, which includes the effect of axial compression. By comparing with the 86 columns, the proposed equation showed a clear trend between the reserve shear strength and the ratio of provided to a required amount of shear reinforcement. Moreover, the proposed equation indicated that all the columns with unacceptable failure modes did not have a sufficient amount of shear reinforcement for successful redistribution of internal forces at diagonal cracking.

Appendix. Test Database of Shear-Critical High-Strength Columns

Major design parameters of shear-critical high-strength columns.

References	Column	f'_c (MPa)	f_{yt} (MPa)	f_{yl} (MPa)	$\frac{N_u}{A_g f'_c}$ (%)	b_w (mm)	h (mm)	d (mm)	a/d	ρ_l (%)	ρ_t (%)	ρ_w (%)	Reserve strength ratio	$\frac{\rho_t}{\rho_{t,minACI}}$	$\frac{\rho_t}{\rho_{t,min,p}}$
Sakaguchi et al. (1990)	C1	93.5	0	957	0.39	400	400	320	1.25	2.14	0.00	0.89	1.00	—	—
	C2	93.5	1,360	957	0.39	400	400	320	1.25	2.14	0.16	0.89	1.10	1.45	0.31
	C4	77	1,400	957	0.24	400	400	320	1.25	2.14	0.40	0.89	1.43	4.04	1.32
	C5	93.5	1,400	957	0.39	400	400	320	1.25	2.14	0.40	0.89	1.26	3.67	0.78
	C6	77	1,400	957	0.48	400	400	320	1.25	2.14	0.40	0.89	1.14	4.04	0.79
	C7	93.5	1,400	957	0.39	400	400	320	1.25	2.14	0.62	0.89	1.32	5.64	1.20
	C8	93.5	1,400	957	0.39	400	400	320	1.25	2.14	0.80	0.89	1.37	7.34	1.56

References	Column	f'_c (MPa)	f_{yt} (MPa)	f_{yl} (MPa)	$\frac{N_u}{A_g f'_c}$ (%)	b_w (mm)	h (mm)	d (mm)	a/d	ρ_l (%)	ρ_t (%)	ρ_w (%)	Reserve strength ratio	$\frac{\rho_t}{\rho_{t,minACI}}$	$\frac{\rho_t}{\rho_{t,min,p}}$
Maruta (2008)	H-0.6-0.15	128	1,053	1,030	0.15	200	200	160	1.25	3.80	0.60	1.58	1.93	4.70	1.77
	H-0.6-0.3	125	1,053	1,030	0.30	200	200	160	1.25	3.80	0.60	1.58	1.41	4.76	1.11
	H-0.6-0.6	120	1,053	1,030	0.60	200	200	160	1.25	3.80	0.60	1.58	1.12	4.86	0.65
	HS-0.6-0.3	128	1,053	1,030	0.30	200	200	160	1.25	3.80	0.60	1.58	1.24	4.70	1.09
	HS-0.6-0.6	128	1,053	1,030	0.60	200	200	160	1.25	3.80	0.60	1.58	1.14	4.70	0.61
	HS-1.2-0.6	129	1,053	1,030	0.60	200	200	160	1.25	3.80	1.20	1.58	1.10	9.37	1.22
	H-0.3-0.6	128	1,053	1,030	0.60	200	200	160	1.25	3.80	0.30	1.58	1.13	2.35	0.31
	H-1.2-0.6	121	1,053	1,030	0.60	200	200	160	1.25	3.80	1.20	1.58	1.23	9.68	1.30
	H-1.8-0.6	130	1,053	1,030	0.60	200	200	160	1.25	3.80	1.80	1.58	1.32	14.00	1.82
	H-0.3-0.3	130	1,053	1,030	0.30	200	200	160	1.25	3.80	0.30	1.58	1.33	2.33	0.54
	H-1.2-0.3	121	1,053	1,030	0.30	200	200	160	1.25	3.80	1.20	1.58	1.95	9.68	2.28
	H-1.8-0.3	121	1,053	1,030	0.30	200	200	160	1.25	3.80	1.80	1.58	1.82	14.52	3.43
	U-0.4-0.6	130	1,450	1,030	0.60	200	200	160	1.25	3.80	0.40	1.58	1.06	3.11	0.40
	U-0.7-0.6	129	1,450	1,030	0.60	200	200	160	1.25	3.80	0.70	1.58	1.11	5.47	0.71
Takami and Yoshioka (1997)	No. 1	99	757	999	0.13	250	250	200	1.25	3.80	0.51	1.58	1.51	4.55	2.01
	No. 2	99	757	999	0.32	250	250	200	1.25	3.80	0.51	1.58	1.34	4.55	1.11
	No. 3	99	757	999	0.51	250	250	200	1.25	3.80	0.51	1.58	1.30	4.55	0.76
	No. 5	99	757	999	0.13	250	250	200	1.25	3.80	1.02	1.58	2.11	9.11	4.02
	No. 6	99	757	999	0.32	250	250	200	1.25	3.80	1.02	1.58	1.44	9.11	2.21
	No. 7	99	757	999	0.51	250	250	200	1.25	3.80	1.02	1.58	1.37	9.11	1.53
Takaine et al. (2010)	H20A-U045s-C-1	188	1,334	1,106	0.30	200	200	160	1.25	5.70	0.45	2.67	1.42	2.91	0.58
	H20A-U045s-0.6C-1	198	1,334	1,106	0.60	200	200	160	1.25	5.70	0.45	2.67	1.11	2.84	0.31
	H20A-U045s-C-1.25	200	1,313	1,106	0.30	450	450	360	1.56	3.40	0.45	0.88	1.00	2.82	0.55
	H20A-U045s-0.6C-1.25	205	1,313	1,106	0.60	450	450	360	1.56	3.40	0.45	0.88	1.02	2.79	0.30
Kuramoto and Minami (1992)	C61	113.8	407	736	0.17	300	300	240	1.88	3.80	1.19	1.58	1.87	7.32	2.67
	C62	113.8	735	736	0.17	300	300	240	1.88	3.80	0.53	1.58	1.50	4.41	1.61
	C63	113.8	766	736	0.17	300	300	240	1.88	3.80	1.19	1.58	1.86	9.90	3.61
	C31	113.8	407	736	0.33	300	300	240	1.88	3.80	1.19	1.58	1.17	7.32	1.63
	C32	113.8	735	736	0.33	300	300	240	1.88	3.80	0.53	1.58	1.14	4.41	0.98
	C33	113.8	766	736	0.33	300	300	240	1.88	3.80	1.19	1.58	1.32	9.90	2.21
Aoyama (2001)	6-1	73.5	402	757	0.17	300	300	240	1.88	3.80	0.53	1.58	1.33	4.01	1.67
	6-2	73.5	409	757	0.17	300	300	240	1.88	3.80	1.19	1.58	1.56	9.16	3.81
	6-3	73.5	934	757	0.17	300	300	240	1.88	3.80	0.53	1.58	1.63	5.48	2.28
	6-4	73.5	1,091	757	0.17	300	300	240	1.88	3.80	1.19	1.58	1.66	12.31	5.13
	3-1	73.5	402	757	0.33	300	300	240	1.88	3.80	0.53	1.58	1.12	4.01	1.05
	3-2	73.5	409	757	0.33	300	300	240	1.88	3.80	1.19	1.58	1.41	9.16	2.41
	3-3	73.5	934	757	0.33	300	300	240	1.88	3.80	0.53	1.58	1.23	5.48	1.44
	3-4	73.5	1,091	757	0.33	300	300	240	1.88	3.80	1.19	1.58	1.49	12.31	3.24
Shinohara et al. (2008)	HRC-0.39-0.10	98	1,425	1,034	0.10	200	250	200	1.50	3.17	0.39	1.98	1.62	3.49	1.77
	HRC-0.39-0.28	121	1,425	1,034	0.28	200	250	200	1.50	3.17	0.39	1.98	1.19	3.15	0.78
	HRC-0.39L-0.28	109	596	1,034	0.28	200	250	200	1.50	3.17	0.39	1.98	1.13	3.31	0.86
	HRC-0.78-0.10	98	1,342	1,034	0.10	200	250	200	1.50	3.17	0.78	1.98	2.84	6.99	3.55
	HRC-0.78-0.28	122	1,342	1,034	0.28	200	250	200	1.50	3.17	0.78	1.98	1.93	6.26	1.55
Akihiko et al. (1990)	CA12-6-1	114	406	736	0.17	300	300	240	1.88	3.80	1.19	1.58	1.84	7.32	2.67
	CA12-6-2	114	734	736	0.17	300	300	240	1.88	3.80	0.53	1.58	1.58	4.41	1.61
	CA12-6-3	114	765	736	0.17	300	300	240	1.88	3.80	1.19	1.58	1.74	9.90	3.61
	CA12-3-1	114	406	736	0.33	300	300	240	1.88	3.80	1.19	1.58	1.14	7.32	1.63
	CA12-3-2	114	734	736	0.33	300	300	240	1.88	3.80	0.53	1.58	1.13	4.41	0.98
	CA12-3-3	114	765	736	0.33	300	300	240	1.88	3.80	1.19	1.58	1.33	9.90	2.21
Sibata et al. (1997)	B-12	118	870	685	0.30	300	300	240	1.88	3.52	0.20	1.37	1.20	1.64	0.39
	B-13	118	870	685	0.30	300	300	240	1.88	3.52	0.40	1.37	1.16	3.27	0.78
	B-14	118	870	685	0.30	300	300	240	1.88	3.52	0.80	1.37	1.12	6.54	1.56
	B-15	118	870	685	0.30	300	300	240	1.88	3.52	1.14	1.37	1.36	9.32	2.22
	B-16	118	870	685	0.30	300	300	240	1.25	3.52	0.40	1.37	1.26	3.27	0.78
Ou and Kurniawan (2015b)	A-1	92.5	862	735	0.10	600	600	480	1.88	3.52	0.16	1.37	1.25	1.30	0.67
	A-2	103.2	862	735	0.10	600	600	480	1.88	3.52	0.16	1.37	1.27	1.23	0.62
	A-3	96.9	862	735	0.10	600	600	480	1.88	3.52	0.28	1.37	1.39	2.20	1.12
	A-4	107.1	862	735	0.10	600	600	480	1.88	3.52	0.28	1.37	1.37	2.09	1.04
	B-1	108.3	862	735	0.15	600	600	480	1.88	3.52	0.16	1.37	1.12	1.20	0.48
	B-2	125.0	862	735	0.18	600	600	480	1.88	3.52	0.16	1.37	1.14	1.12	0.37
	B-3	112.8	862	735	0.20	600	600	480	1.88	3.52	0.28	1.37	1.15	2.03	0.66
	B-4	121.0	862	735	0.20	600	600	480	1.88	3.52	0.28	1.37	1.20	1.96	0.62

Appendix. (*Continued.*)

References	Column	f'_c (MPa)	f_{yt} (MPa)	f_{yl} (MPa)	$\frac{N_u}{A_g f'_c}$ (%)	b_w (mm)	h (mm)	d (mm)	a/d	ρ_l (%)	ρ_t (%)	ρ_w (%)	Reserve strength ratio	$\frac{\rho_t}{\rho_{t,minACI}}$	$\frac{\rho_t}{\rho_{t,min,p}}$
Ou and Kurniawan (2015a)	C-1	104.1	862	735	0.30	600	600	480	1.88	3.52	0.16	1.37	1.00	1.22	0.31
	C-2	138.8	862	735	0.30	600	600	480	1.88	3.52	0.16	1.37	1.00	1.06	0.24
	C-3	104.6	862	735	0.30	600	600	480	1.88	3.52	0.28	1.37	1.03	2.11	0.53
	C-4	130.0	862	735	0.30	600	600	480	1.88	3.52	0.28	1.37	1.00	1.90	0.44
	D-1	101.0	862	735	0.40	600	600	480	1.88	3.52	0.16	1.37	1.00	1.24	0.25
	D-2	125.5	862	735	0.40	600	600	480	1.88	3.52	0.16	1.37	1.00	1.11	0.21
	D-3	106.4	862	735	0.40	600	600	480	1.88	3.52	0.28	1.37	1.00	2.09	0.42
	D-4	127.8	862	735	0.40	600	600	480	1.88	3.52	0.28	1.37	1.00	1.91	0.35
This research	A-3.1	92.2	862	735	0.10	600	600	480	1.88	3.38	0.28	1.23	1.31	2.25	1.16
	A-6	90.8	862	735	0.10	600	600	480	1.88	3.38	0.65	1.23	1.85	5.24	2.71
	B-3.1	78.0	862	735	0.20	600	600	480	1.88	3.38	0.28	1.23	1.00	2.45	0.90
	B-5	78.0	862	735	0.20	600	600	480	1.88	3.38	0.46	1.23	1.09	3.98	1.46
	B-6	101.1	862	735	0.20	600	600	480	1.88	3.38	0.65	1.23	1.30	4.97	1.67
	C-5	79.6	862	735	0.30	600	600	480	1.88	3.38	0.46	1.23	1.00	3.94	1.09
	C-6	80.3	862	735	0.30	600	600	480	1.88	3.38	0.65	1.23	1.13	5.58	1.53
	D-5	82.8	862	735	0.40	600	600	480	1.88	3.38	0.46	1.23	1.00	3.86	0.85
	D-6	84.9	862	735	0.40	600	600	480	1.88	3.38	0.65	1.23	1.08	5.42	1.18

Data Availability Statement

Some or all data, models, or code generated or used during the study are available from the corresponding author by request. (Lateral force and displacement relationships)

Acknowledgments

The authors would like to thank the financial support from the Ministry of Science and Technology of Taiwan under Contract Nos. 107-2625-M-002-010 and from the National Center for Research on Earthquake Engineering (NCREE) of Taiwan.

Notation

The following symbols are used in this paper:

A_g = gross area of concrete cross section;
$A_{v,min,p}$ = proposed minimum area of shear reinforcement;
$A_{v,minACI}$ = minimum area of shear reinforcement specified by ACI 318-19;
a = shear span;
b_w = web width of member cross section;
d = effective depth of member cross section, which is taken as 80% h;
f'_c = concrete compressive strength;
f_{yl} = yield strength of longitudinal reinforcement;
f_{yt} = yield strength of shear reinforcement;
h = overall height of member cross section;
N_u = applied axial load (positive in compression);
s = spacing of shear reinforcement;
V_c = nominal shear strength provided by concrete;
V_{Mn} = shear corresponding to the flexural strength;
V_{test_d} = experimental shear strength at diagonal cracking condition;
V_{test_u} = experimental shear strength at ultimate condition (peak load);
α = reserve shear strength ratio (V_{test_u}/V_{test_d});
ρ_l = longitudinal reinforcement ratio;
ρ_t = shear reinforcement ratio;
$\rho_{t,minACI}$ = minimum shear reinforcement ratio specified by ACI 318-19;
$\rho_{t,min,p}$ = proposed minimum shear reinforcement ratio;
ρ_w = longitudinal tension reinforcement ratio;
σ_{yl} = maximum stress in longitudinal reinforcement; and
σ_{yt} = maximum stress in shear reinforcement.

References

ACI (American Concrete Institute). 2019. *Building code requirements for structural concrete*. ACI 318. Farmington Hills, MI: ACI.

Akihiko, N., H. Kuramoto, and M. Koichi. 1990. "Shear strength and behavior of reinforced concrete columns using high-strength concrete of $\sigma_B = 1200\ \mathrm{kgf/cm^2}$ (Part 1 & Part 2)." In *Proc., Architectural Institute of Japan*, 53–56. Tokyo: Architectural Institute of Japan.

Aoyama, H. 2001. *Design of modern highrise reinforced concrete structures*. Singapore: World Scientific.

Kuramoto, H., and K. Minami. 1992. "Experiments on the shear strength of ultra-high strength reinforced concrete columns." In *Proc., 10th World Conf. on Earthquake Engineering*, 3001–3006. Cleveland: CRC Press.

Kuwada, H., A. Nakayama, and K. Minami. 1993. "Shear strength of reinforced concrete columns using high strength concrete of $\sigma_B = 600\ \mathrm{kgf/cm^2}$." *Proc. Jpn. Concr. Inst.* 15 (2): 473–478.

Lee, J. Y., I. J. Choi, and S. W. Kim. 2011. "Shear behavior of reinforced concrete beams with high-strength stirrups." *ACI Struct. J.* 108 (5): 620–629.

Lee, J.-Y., D. H. Lee, J.-E. Lee, and S.-H. Choi. 2015. "Shear behavior and diagonal crack width for reinforced concrete beams with high-strength shear reinforcement." *ACI Struct. J.* 112 (3): 323–333. https://doi.org/10.14359/51687422.

Maruta, M. 2008. "Shear capacity of reinforced concrete column using high strength concrete." In *Proc., 8th Int. Symp. on Utilization of High-Strength and High-Performance Concrete*. Tokyo: Japan Concrete Institute and Japan Prestressed Concrete Engineering Association.

Munikrishna, A., A. Hosny, S. Rizkalla, and P. Zia. 2011. "Behavior of concrete beams reinforced with ASTM A1035 Grade 100 stirrups under shear." *ACI Struct. J.* 108 (1): 34–41.

Ou, Y.-C., and D. P. Kurniawan. 2015a. “Effect of axial compression on shear behavior of high-strength reinforced concrete columns.” *ACI Struct. J.* 112 (2): 209–220. https://doi.org/10.14359/51687300.

Ou, Y.-C., and D. P. Kurniawan. 2015b. “Shear behavior of reinforced concrete columns with high-strength steel and concrete.” *ACI Struct. J.* 112 (1): 35–45. https://doi.org/10.14359/51686822.

Sakaguchi, N., K. Yamanobe, Y. Kitada, T. Kawachi, and S. Koda. 1990. “Shear strength of high-strength concrete members.” In *Proc., SP-121: 2nd Int. Symp. on High-Strength Concrete*, 155–178. Farmington Hills, MI: American Concrete Institute.

Seo, M., and H. Noguch. 1992. “Experimental study on shear behavior of RC columns using high-strength materials (Part 1 and Part 2).” In *Proc., Summary of Technical Papers of Annual Meeting, Structure II*, 627–630. Tokyo: Architectural Institute of Japan.

Shinohara, Y., T. Kubota, and S. Hayashi. 2008. “Shear crack behaviors of ultra-high-strength concrete columns (Part 1 & Part 2).” In *Proc., Summaries of Technical Papers of Annual Meeting, Structures IV*, 605–608. Tokyo: Architectural Institute of Japan.

Sibata, M., H. Kanasugi, M. Uwada, H. Ooyama, and Y. Yamashita. 1997. “Experimental study on shear behavior of reinforced concrete columns using high-strength shear reinforcement of 8000 $\mathrm{kgf/cm^2}$ Grade (Part 4).” In *Proc., Summaries of Technical Papers of Annual Meeting, Structures IV*, 7–8. Tokyo: Architectural Institute of Japan.

Takaine, Y., S. Nagai, M. Maruta, and N. Suzuki. 2010. “Shear performance of RC column using 200 $\mathrm{N/mm^2}$ concrete.” In *Proc., Summaries of Technical Papers of Annual Meeting, Structures IV*, 295–296. Tokyo: Architectural Institute of Japan.

Takami, S., and K. Yoshioka. 1997. “Shear strength of RC columns using high-strength concrete.” In *Proc., Summaries of Technical Papers of Annual Meeting, Structures IV*, 25–26. Tokyo: Architectural Institute of Japan.